



Soy protein interactions with polyphenols: Structural and functional changes in natural and cationized forms

Shizhang Yan, Qi Wang, Jiaye Yu, Yang Li, Baokun Qi*

College of Food Science, Northeast Agricultural University, Harbin, Heilongjiang 150030, China

ARTICLE INFO

Keywords:

Soy protein isolate
Gallic acid
Cationic soybean protein isolate
Phenolic binding
Functional property

ABSTRACT

Herein, cationic soy protein (NSPI) was synthesized by grafting Ethylenediamine (EDA) onto soy protein isolate (SPI), and protein–gallic acid (GA) complexes were formed by mixing NSPI with GA in various ratios. We assessed the structure, particle size, thermal stability, emulsifying ability, and antioxidant capacity of NSPI and complexes. Results show that grafting with EDA introduced a positive charge to SPI and resulted in a uniform particle size, and enhanced thermal stability, emulsifying ability, and antioxidant capacity. In addition, NSPI presented more amino groups and stronger interactions with GA compared to SPI. EDA and GA synergistically increased the flexibility of SPI, reducing the α -helix content and increasing the random coil content. Moreover, the interactions between SPI, NSPI, and GA were static, and hydrophobic and electrostatic between GA and SPI and NSPI, respectively. Grafting SPI with EDA improved functionality and interactions with GA, implying that NSPI-GA complexes may function as emulsifiers and antioxidants.

1. Introduction

Recently, the mechanism underlying the interaction between dietary proteins and phenolic compounds has garnered considerable interest, primarily because of their widespread use in the food industry. Dietary proteins and phenolic compounds are often co-present in foods, such as soymilk, milk, and plant-based vegetarian meat (Zhang et al., 2021). Additionally, it has also been shown that dietary proteins and phenolic compounds can readily interact to form noncovalent/covalent complexes (Yan, Xie, Zhang, Jiang, et al., 2021). Specifically, dietary proteins can serve as natural carriers for phenolic compounds via mutual interactions. This interaction modifies the structure and function of proteins and enhances the stability and bioavailability of the bound substances (Chen et al., 2019; Yan, Xu, Zhang, Xie, et al., 2021). Therefore, it is important to explore and develop relevant systems to elucidate the binding mechanisms.

Soybean protein isolate (SPI), an important plant protein, is widely used in the food and pharmaceutical industries because of its low cost, high nutritional value, and good biocompatibility and biodegradability (Yan, Xu, Zhang, & Li, 2021). For example, it is commonly added to commercial foods and beverages, such as infant formula, functional drinks, and fermented milk (Dai et al., 2023). In addition, studies have shown that SPI can interact with phenolic compounds and induce

structural changes in the protein. These changes are closely related to the functional, nutritional, and even sensitivity of the formed complex (Pi, Liu, et al., 2023). Gallic acid (GA), a structurally simple, plant-derived polyphenol, contains two *ortho*-phenol groups, a *para*-phenol group, and a carboxylic acid group, which provide it with biological activity, including antioxidant, antibacterial, and anticancer properties. Therefore, researchers have combined GA with SPI to produce proteins with antibacterial and anti-inflammatory properties (Yi et al., 2021). For example, H. Wang et al., (2022) showed that GA can induce conformational changes in proteins and endow them with antioxidant properties. Furthermore, Yan et al., (2022) used GA to modify soy protein, finding that it effectively retarded protein oxidation at the oil–water interface.

To date, many studies have been conducted on the interactions between SPI and different polyphenols, which enhance the solubility, stability, and bioavailability of target compounds, as well as enabling controlled release (Dai et al., 2023; Pi, Sun, et al., 2023; Wang et al., 2022; Yi et al., 2021). However, it is generally accepted that the successful delivery of polyphenols by proteins is highly dependent on the surface properties of the encapsulating material, such as charge and hydrophobicity (Teng et al., 2014). For example, Likitdechajaroj & Ratanavaraporn (2018) prepared ethylenediamine coupled cationic gelatin and succinic anhydride coupled anionic gelatin and compared

* Corresponding author.

E-mail address: qibaokun22@163.com (B. Qi).

<https://doi.org/10.1016/j.fochx.2023.100866>

Received 20 July 2023; Received in revised form 20 August 2023; Accepted 5 September 2023

Available online 6 September 2023

2590-1575/© 2023 The Author(s). Published by Elsevier Ltd. This is an open access article under the CC BY-NC-ND license (<http://creativecommons.org/licenses/by-nc-nd/4.0/>).

their ability to stabilize the emulsion and load EGCG. The results demonstrated that cationic gelatin extends the release duration of EGCG due to its ion attraction to negatively charged EGCG and improved capacity to produce emulsified microspheres. Similarly, Tan et al., (2022) modified gelatin using ethylenediamine and discovered that it had higher hydrophobicity, emulsification properties, and antioxidant properties compared with natural gelatin. This aspect enabled the effective stabilization of pickering emulsions and improved oxidative stability of the emulsions and retention of encapsulated β -carotene. Furthermore, Zhou et al., (2022) also showed that cationic soybean anionic polysaccharides can improve the stability of epigallocatechin gallate (EGCG) and ensure its continuous release. Therefore, the cationic treatment of SPI could be a suitable method for improving the delivery of phenolic substances.

This study assumes that cationic soybean protein isolate (NSPI) has better functional properties and can bind to gallic acid (GA) more effectively than soybean protein isolate (SPI). Therefore, this research objectives were: (1) the carbodiimide-mediated grafting of ethylenediamine (EDA) to an SPI, synthesizing an NSPI and investigating its changes in structure and function; (2) to investigate the binding mechanism NSPI with GA, a polyphenolic compound and, thus, explore the potential of NSPI as a carrier and enhancer of bioactive components. This study provides new insights into developing novel delivery systems with the required properties and an understanding of the interaction mechanisms between proteins and polyphenols.

2. Materials and methods

2.1. Materials

The SPI was prepared using alkaline dissolution and acid precipitation, as described by us previously (Yan et al., 2022). GA (>98%), 1-ethyl-3-(3-dimethylaminopropyl) carbodiimide hydrochloride (EDC), *N*-hydroxysuccinimide, *o*-phthalaldehyde (OPA), and 5,5'-dithiobis(2-nitrobenzoic acid) (DTNB) were purchased from Shanghai Yuanye Biochemical (Shanghai, China). Urea, hydrochloric acid, and sodium hydroxide were purchased from Solabao (Beijing, China). All reagents were analytically pure.

2.2. Amination of SPI

SPI was modified with EDA according to a previously reported method (Sarika & James, 2016). Briefly, 5 g of SPI was dissolved in 50 mL of phosphate buffered saline (PBS; 10 mM, pH 5.0), and 2.68 g (0.017 mol) of 1-ethyl-3-(3-dimethylaminopropyl) carbodiimide (EDC) was added. The reaction was carried out for 1 h. In addition, 15.8 mL (0.23 mol) of EDA was added, and the pH was adjusted to 5 with 6 mol HCl in an ice-water bath. The protein solution was mixed with the EDA solution and stirred at room temperature for 20 h. Then, a dialysis bag (MWCO: 3000 Da) was used for dialysis in distilled water for 48 h. Aminated SPI was obtained by freeze-drying and denoted NSPI.

2.3. Preparation of protein-polyphenol complex

A 1 g sample of protein was weighed out and dissolved in deionized water (100 mL), followed by hydration at 4 °C for 24 h to ensure its full dissolution. Then, GA was added to the protein solution in a protein-to-GA ratio of 20:1 (w/w). Next, the sample was mixed at 25 °C for 24 h, and cooled to -20 °C for pre-freezing and freeze-dried using a vacuum freeze-dryer. SPI and GA complexes are denoted SPI-GA, and those of NSPI and GA are named NSPI-GA.

2.4. Determination of particle size and zeta potential

A sample solution having a concentration of 0.5 mg/mL was prepared, and a particle size analyzer (Nano-Z, Malvern Worcestershire,

UK) was used to determine the particle size and ζ -potential of the samples. The refractive indices of the particles and dispersant were 1.46 and 1.33, respectively, while the absorption parameter was 0.001. The loading volume, measurement temperature, and temperature equilibration time were 1 mL, 25 °C, and 2 min, respectively.

2.5. Degree of substitution by EDA

The elemental compositions of SPI and NSPI were determined using a cube elemental analyzer (Vario EL, Elemental, Germany). The degree of amination of the NSPI was calculated using the changes in nitrogen content (Chen et al., 2022).

2.6. Analysis of reactive group content

2.6.1. Determination of free amino content

OPA solution was prepared as follows: 80 mg of OPA in 2 mL methanol, 5 mL aqueous sodium dodecyl sulfate (SDS) solution (2%), 50 mL aqueous sodium borate solution (0.1 M), and 200 mL of β -mercaptoethanol were combined and made up to 100 mL with deionized water. Then, 200 μ L of the protein sample (0.5 mg mL⁻¹) was mixed with 4 mL of the OPA solution and incubated at 35 °C for 2 min. Finally, the absorbance at 340 nm was measured, and the amino acid content in the sample was calculated by constructing a standard curve using L-leucine.

2.6.2. Determination of sulfhydryl content

Each sample (10 mg) was added to Tris-glycine reagent (10 mL, containing 0.086 M Tris, 0.09 M glycine, 4 mM ethylenediaminetetraacetic acid sodium (Na₂EDTA), and 8 M urea) to prepare a solution with a concentration of 1 mg mL⁻¹. Then, 200 μ L of DTNB solution (4 mg mL⁻¹ dissolved in Tris-glycine buffer) was maintained in the dark at 25 °C for 30 min. Finally, a UV-Vis spectrophotometer was used to measure the absorbance at 412 nm, and the sulfhydryl content was calculated using the following Eq. (1):

$$\text{Sulfhydryl (nmol/mg sample)} = A_{412} \times 73.53/C \quad (1)$$

where *C* is the concentration of the sample, and *A*₄₁₂ is the absorbance of the sample solution at 412 nm.

2.7. Ultraviolet – visible spectroscopy

A sample was dissolved in deionized water to yield a sample solution having a concentration of 0.5 mg mL⁻¹, and a UV visible spectrophotometer (Lambda 35, PerkinElmer) was used to record the UV spectrum of the sample between 200 and 600 nm at medium scanning speed in intervals of 0.2 nm.

2.8. Fourier transform infrared spectroscopy (FT-IR)

A sample was combined with KBr (1:100 w/w ratio), made into a tablet, and the spectrum was collected using a Nicolet 6700 FT-IR spectrometer (Thermo Scientific Instrument) between 4000 and 400 cm⁻¹ using 64 scans at a resolution of 2 cm⁻¹.

2.9. X-ray diffraction analysis

The crystallinity of the sample was analyzed using an X'pert powder X-ray diffractometer (PANalytical The Netherlands) equipped with a Cu radiation source. X-rays were generated at 40 kV and 40 mA. The XRD patterns were collected between 2 θ of 5° and 90°.

2.10. Intrinsic fluorescence spectrum

Fluorescence spectra of the protein and protein-polyphenol complexes (0.5 mg mL⁻¹) were measured using an F-6000 fluorescence

spectrometer (Hitachi Ltd., Tokyo, Japan). In addition, we determined the binding affinities between the proteins and polyphenols. A 10 mL protein solution (0.5 mg mL⁻¹) was mixed with an aliquot of GA (0–30 μmol) in a 10-mL test tube. The mixture was incubated at 25 °C for 10 min, and then centrifuged at 2000g for 10 min to collect the supernatant. Measurements were performed at an excitation wavelength of 280 nm, with emission wavelengths in the range of 300–450 nm. The width of both the emission and excitation slits was 5 nm. The values of the Stern–Volmer burst constant (K_{sv}), fluorescence burst rate constant (K_q), K_a (binding constant), and number of binding sites (n) were obtained from the following Eqs. (2) and (3) (Yan, Xu, Zhang, Xie, et al., 2021).

$$\frac{F_0}{F} = 1 + K_{sv}[Q] = 1 + K_q\tau_0[Q] \quad (2)$$

$$\lg\left[\frac{F_0 - F}{F}\right] = n\lg[Q] + \lg K_a \quad (3)$$

Here, F_0 and F respectively represent the maximum fluorescence intensity with or without GA, respectively, and $[Q]$ represents the concentration of the GA, and τ_0 (10⁻⁸s) is the lifespan of the quenching agent.

The thermodynamic parameters were calculated using the Van't Hoff Eqs. (4) and (5):

$$\ln K_a = \frac{-\Delta H}{RT} + \frac{\Delta S}{R} \quad (4)$$

$$\Delta G = \Delta H - T\Delta S \quad (5)$$

Here, ΔG , ΔH , and ΔS are the change in free energy, enthalpy, and entropy, respectively, R is the gas constant (8.314 J mol⁻¹ K⁻¹), and T is the experimental temperature.

2.11. DSC analysis

The thermal denaturation temperature (T_d) of the samples was evaluated using DSC (DSC 8000, PerkinElmer, USA) between 25 and 250 °C. The heating rate was 10 °C min⁻¹ in a nitrogen atmosphere (50 mL min⁻¹).

2.12. Determination of surface hydrophobicity

The surface hydrophobicity of the protein and its complex was measured using the fluorescent probe 1-anilino-8-naphthalene sulfonate (ANS). Briefly, the sample solution (6 mL, 0.5 mg mL⁻¹) was mixed with an ANS solution (120 μL, 8 mM), and the fluorescence intensity was measured using an F-6000 fluorescence spectrometer (Hitachi, Tokyo, Japan) at an excitation wavelength of 365 nm and an emission wavelength of 400–600 nm. The slit size was 5 nm. The maximum fluorescence intensity was used to evaluate the hydrophobicity of sample surfaces.

2.13. Determination of emulsification characteristics

To prepare the emulsion, 25 mL of the sample solution (1 mg mL⁻¹) and 5 mL of soybean oil were homogenized at 12,000 rpm for 3 min (T-25; IKA, Staufen, Germany). Then, 50 μL of the emulsion was mixed with 10 mL of 0.1% SDS and its absorbance at 500 nm was measured at 0 and 10 min. The emulsifying activity (EA) was the absorbance at 0 min, and the emulsion stability (ES) was calculated as (Eq. (6)):

$$ES (\text{min}) = \frac{A_0 \times 100}{A_0 - A_{10}} \quad (6)$$

where A_0 and A_{10} are the absorbances at 0 and 10 min, respectively.

2.14. Determination of antioxidant activity

A fresh solution of 0.1 mM of 2,2-diphenyl-1-picrylhydrazine (DPPH) was prepared and stored in the dark for 3 h before use. Before sample analysis, the DPPH solution was diluted with anhydrous ethanol to an absorbance of <0.7. Then, 2 mL of the aqueous sample solution (1 mg mL⁻¹) were mixed with an equal volume of DPPH solution. The mixture was immediately placed in the dark, and its absorbance was measured at 517 nm using a UV spectrophotometer after 30 min. Anhydrous ethanol was used as the blank control, and the DPPH radical clearance rate was calculated according to the following Eq. (7) (Yan et al., 2022):

$$DPPH \text{ free radical scavenging rate} = 1 - \frac{A}{A_0} \times 100\% \quad (7)$$

Here, A and A_0 represent the absorbance of the sample and blank at 517 nm, respectively.

A 7 mM 2,2-azido bis(3-ethyl benzothiazole line-6-sulfonic acid) (ABTS) solution and a 2.45 mM potassium persulfate aqueous solution were mixed in equal volumes and stored in the dark for 12–16 h at 25 °C. Before analysis, the ABTS working solution was diluted with PBS (pH 7.2, 10 mM) to an absorbance of 0.70 ± 0.02. The sample solution was mixed with the ABTS working solution in equal volumes and allowed to react in the dark for 30 min. The absorbance was measured at 734 nm using a spectrophotometer with PBS as a blank. The free radical clearance rate of ABTS was calculated as follows (Eq. (8)):

$$ABTS \text{ free radical scavenging rate} = 1 - \frac{A}{A_0} \times 100\% \quad (8)$$

where A and A_0 represent the absorbance of the sample and blank at 734 nm, respectively.

2.15. Statistical analysis

The experiments were performed in triplicate and the results are expressed as mean ± standard deviation. One-way analysis of variance (ANOVA) and Duncan's test were used for statistical analysis by the SPSS 26.0 software package (SPSS Inc., Chicago, USA). Differences were considered significant at $p < 0.05$. All figures were generated by Origin 2023 (OriginLab Co., USA).

3. Results and discussion

3.1. Analysis of the synthetic mechanism and physicochemical properties

The mechanism of the reaction between SPI and EDA is shown in Fig. 1A. The carboxyl group in SPI was activated by EDC and then polymerized with EDA. As a result of the presence of amino groups in NSPI, the protein carries a positive charge (Sarika & James, 2016). The degree of amination of SPI was approximately 32.6%; these results are consistent with those of Sarika et al. (2015), who found that the degree of amination of gelatin was approximately 37.7%.

To understand the effect of the addition of EDA and the binding of GA on protein properties, the particle size and ζ -potential of the sample were investigated, as shown in Fig. 1B and C. Compared with that of SPI, the particle size distribution of NSPI is almost consistent with that of SPI, with only a small peak appearing at approximately 500 nm, which could be attributed to the self-polymerization of SPI caused by EDC (Wang et al., 2019). After the proteins and polyphenols had been combined, there was a significant change in particle size. For SPI-GA, the change in particle size after combination with GA may be attributed to hydrophobic and hydrogen bonding interactions between the polyphenols and proteins, which act as a bridge for polymerizing protein molecules (Dai et al., 2023; Zhou et al., 2020). The NSPI-GA complex is mainly attributed to the protein being positively charged and prone to electrostatic binding with GA, resulting in the formation of larger

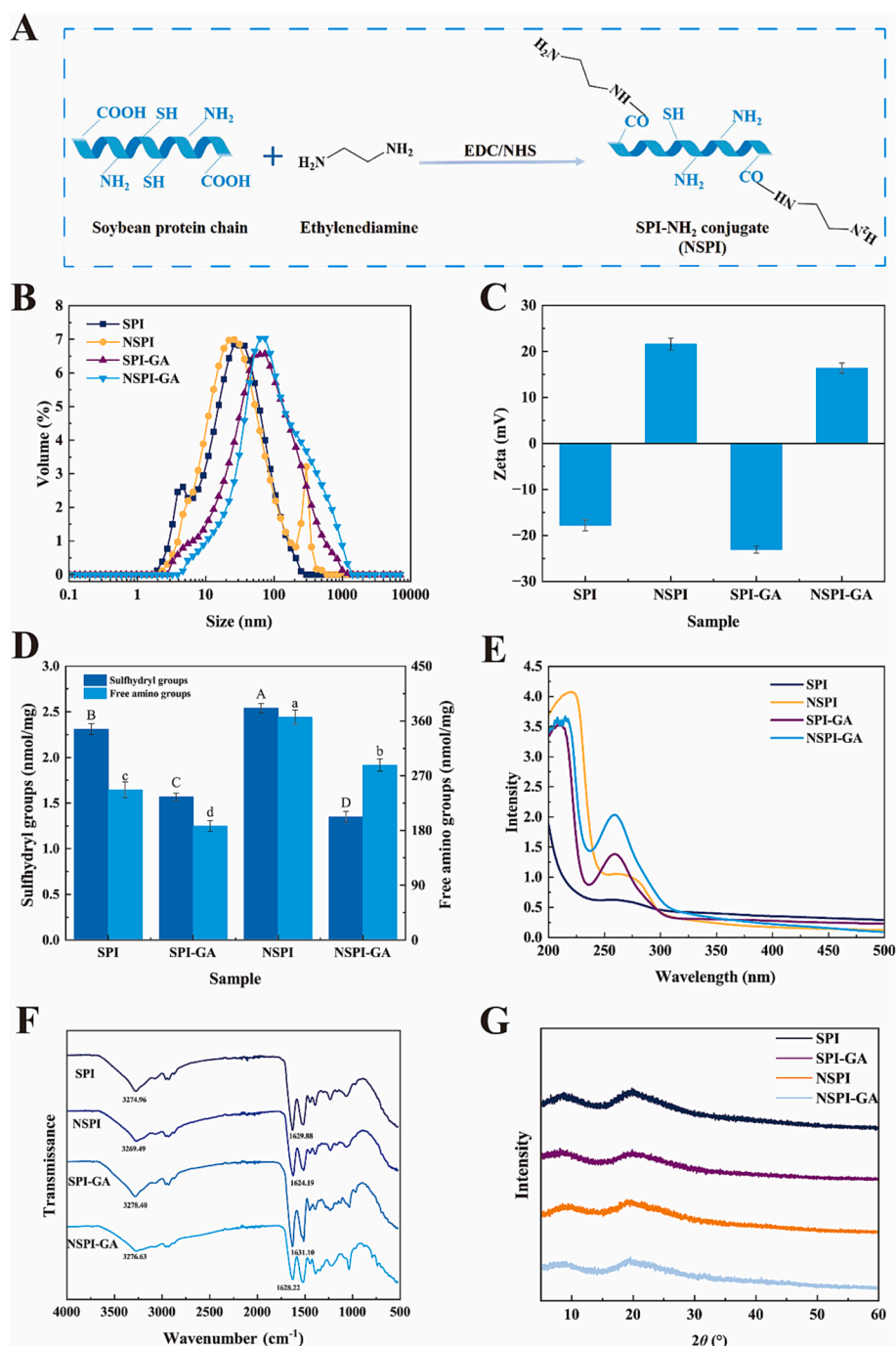


Fig. 1. (A) Reaction mechanism of EDA grafting and GA complexation, (B) particle size distribution of SPI, NSPI, and protein-GA complexes, (C) ζ -potential of SPI, NSPI, and protein-GA complexes, (D) reactive group content of SPI and NSPI, (E) UV spectroscopy of SPI, NSPI, and protein-GA complexes, (F) FT-IR spectra of SPI, NSPI, and protein-GA complexes, and (G) XRD patterns of SPI, NSPI, and protein-GA complexes.

particle complexes (Li et al., 2022). Therefore, the size of the NSPI-GA composite was larger than that of the SPI-GA composite.

The ζ -potentials of the protein and protein-GA complexes are shown in Fig. 1C. Compared to SPI, NSPI has a higher positive charge as a result of the grafting of more positively charged amino groups into the protein (Sarika et al., 2015). After complexation with GA, the SPI-GA complex showed a higher negative charge, which is due to the combination of SPI and a large number of negatively charged GA molecules, which canceled the positive electrostatic charge of the protein (Dai et al., 2023). Similarly, after combination with GA, the positive charge of NSPI-GA decreased because of electrostatic binding between the negatively charged GA and NSPI, thereby reducing the positive charge of the

composite (Chen et al., 2022; Sarika & James, 2016).

3.2. Analysis of reactive group content

Amino and thiol groups in proteins are highly reactive and can be used to characterize the degree of protein modification (Yan et al., 2022). Compared to SPI, the amino and thiol contents of NSPI were higher, possibly because (1) the grafting of EDA significantly increases the amino content of the protein, (2) EDA is strongly alkaline, resulting in protein unfolding during the grafting reaction, and the sulfhydryl group inside the protein exposes or breaks the disulfide bonds of the protein. After compounding with GA, the thiol and amino group

contents in SPI-GA and NSPI-GA decreased significantly, which can be attributed to the interaction between polyphenols and the protein thiol and amino groups. Similar results were reported by Mohammadi et al. (2023), and, taken together, these findings suggest that polyphenols can interact with amino and thiol groups in soybean protein. Interestingly, GA reduced the number of thiol and amino groups in NSPI to a greater extent than that of SPI, indicating a stronger interaction between GA and NSPI. This may be because NSPI has more reaction sites than SPI, as well as an unfolded protein structure.

3.3. UV-vis spectroscopy

The UV-Vis spectra of all samples are shown in Fig. 1E. SPI is a typical protein, and the tryptophan, tyrosine, and phenylalanine residues show characteristic absorption at approximately 280 nm. Compared to that of SPI, the UV absorption peak of NSPI was significantly enhanced and red-shifted, possibly because of changes in the protein secondary structure caused by the exposure of hydrophobic groups embedded in the protein or the increase in amino content (Yan, Xu, Zhang, & Li, 2021). After compounding with GA, the UV absorption spectra of the SPI-GA and NSPI-GA complexes were significantly stronger than those of the proteins and showed a significant blue shift, possibly because of the interaction between proteins and phenolic compounds, which significantly increased the hydroxyl content of the composite material and, thus, enhanced the UV absorption intensity (Wang et al., 2022).

3.4. FT-IR

FT-IR spectroscopy can be used to characterize secondary structural changes in proteins and the interactions between chemical bonds. As shown in Fig. 1F, the spectrum of SPI contains four typical characteristic peaks: 3274.96, 1629.88, 1516.06, and 1234.70 cm^{-1} , corresponding to amide A (hydrogen bonding with N—H stretching), amide I (C=O stretching), amide II (N—H bending), and amide III (C—N stretching and N—H deformation), respectively (Yan, Xu, Zhang, & Li, 2021). Compared with those of SPI, the peaks of NSPI were significantly shifted, especially the amide II and A bands, which were shifted to 1513.93 and 3278.40 cm^{-1} , respectively, indicating that more amide bonds were formed by the grafting of amino groups (Chen et al., 2023). Similar results were also reported by Teng et al. (2014), who reported that the amination of β -lactoglobulin resulted in the formation of more amide bonds. After complexation with GA, the peaks of both SPI and NSPI shifted significantly, indicating that the interactions of the protein with GA caused the structural rearrangement of the protein (Dai et al., 2023). This may be related to the ability of polyphenols to react with the side-chain amino acids of proteins, which is consistent with the results of our reactive group determination. In addition, the intensity of the peak at 1069.58 cm^{-1} significantly increased, and the peak intensity of NSPI-GA was more significant than that of SPI-GA. The band was assigned to the C=O stretching vibration of the phenolic —OH group, further confirming the successful complexation of GA with the protein (Li et al., 2022).

To observe the changes in the secondary structure of the protein in detail, deconvolution of the amide I band was performed and the changes in the α -helix, β -sheet, β -turn, and random coil contents were

Table 1
Secondary structure content of proteins and protein-polyphenol complexes.

Sample	α -helix	β -sheet	β -turn	random coil
SPI	20.34 \pm 0.08 ^a	36.86 \pm 0.14 ^a	23.98 \pm 0.12 ^d	18.97 \pm 0.09 ^d
NSPI	17.29 \pm 0.11 ^c	33.73 \pm 0.16 ^c	26.10 \pm 0.21 ^b	23.87 \pm 0.15 ^b
SPI-GA	18.26 \pm 0.12 ^b	34.82 \pm 0.11 ^b	25.57 \pm 0.15 ^c	22.49 \pm 0.17 ^c
NSPI-GA	15.19 \pm 0.15 ^d	31.09 \pm 0.21 ^d	28.79 \pm 0.16 ^a	26.57 \pm 0.22 ^a

Note: Mean values with different letters (a-d) in the same column indicate statistically significant differences ($p < 0.05$).

calculated (Table 1). Compared with those of SPI, the α -helix and β -sheet content of NSPI decreased and the β -turn and random coil content increased. The decrease in α -helix content could be attributed to the partial unfolding of the α -helix region caused by amine grafting, whereas the increase in random coil content could be attributed to the decrease in the number of intramolecular hydrogen bonds or the unfolding of the SPI molecule and subsequent formation of the random coil structure (Yan, Xu, Zhang, & Li, 2021). In particular, the reduction in the β -sheet content contributes to the exposure of the hydrophobic region of the protein (Zhu et al., 2020). Similar results were also found by Teng et al. (2014), who showed that β -sheets contribute to the hardness and indigestibility of β -lactoglobulin (BLG), and when the cationization of BLG was carried out, the β -sheet content was significantly reduced and the random coil content was significantly increased. After complexation with GA, the α -helix and β -sheet contents of both SPI-GA and NSPI-GA decreased, the random coil content increased, and the secondary structure content of NSPI-GA significantly decreased, indicating that complexation of the protein with GA stretched the structure of the protein and increased its flexibility of the protein structure (Yan et al., 2022). Similar results were reported by Sui et al., (2018), who showed that the complexation of polyphenols with SPI decreased the α -helix content and increased the random coil content of the protein. This change may also be attributed to the consumption of Asp and Glu by GA because both substances are abundant in the β -sheet (Teng et al., 2014).

3.5. XRD

The XRD patterns of the protein and protein-polyphenol complexes are shown in Fig. 1G. SPI produced two broad diffraction peaks at $2\theta = 8.76^\circ$ and 19.9° , which correspond to the α -helix and β -sheet structures of the secondary conformation of the soy protein molecule, respectively (Zeng et al., 2022). In contrast, the intensity of the diffraction peaks in the pattern of NSPI was reduced, and the peaks were slightly shifted compared to that of SPI, indicating that the cationized protein has an amorphous structure, probably because of the reduced α -helix and β -sheet content in the protein, which is consistent with our FT-IR results. Similar results were reported by Sakira and James (2016), who showed that cationization reduces the α -helix content of gelatin, rendering it amorphous. The intensities of the peaks in the XRD patterns of SPI-GA and NSPI-GA were also reduced after complexation with GA compared to those in the pattern of the protein alone, and NSPI-GA had the least intense diffraction peak, suggesting the partial collapse of the crystal structure of the protein molecule, probably because of the noncovalent interactions between the protein and polyphenol, which resulted in a disordered structure and the exposure of hydrophobic functional groups that had been wrapped inside the protein structure (Jin et al., 2020).

3.6. Fluorescence spectroscopy

3.6.1. Intrinsic fluorescence spectra

Intrinsic fluorescence spectroscopy can be used to obtain detailed information about the characteristic conformational changes in proteins (Wang et al., 2021). The fluorescence spectra of SPI, NSPI, and their complexes with GA are shown in Fig. 2A. Compared to that of SPI, the fluorescence intensity of NSPI significantly increased, indicating that amination grafting exposes the hydrophobic groups inside the protein, whereas the side chain groups previously buried inside the protein are exposed to a polar environment, thereby altering the fluorescence properties of the protein. In addition, the maximum emission spectrum of NSPI showed a red shift, which may be due to the expansion of the protein structure, consequently exposing the aromatic amino acids inside the protein to the polar microenvironment, resulting in a high maximum excitation wavelength (Jiang et al., 2009). After combination with GA, the fluorescence intensity of the SPI-GA and NSPI-GA complexes decreased, indicating that the conformation of the peptide

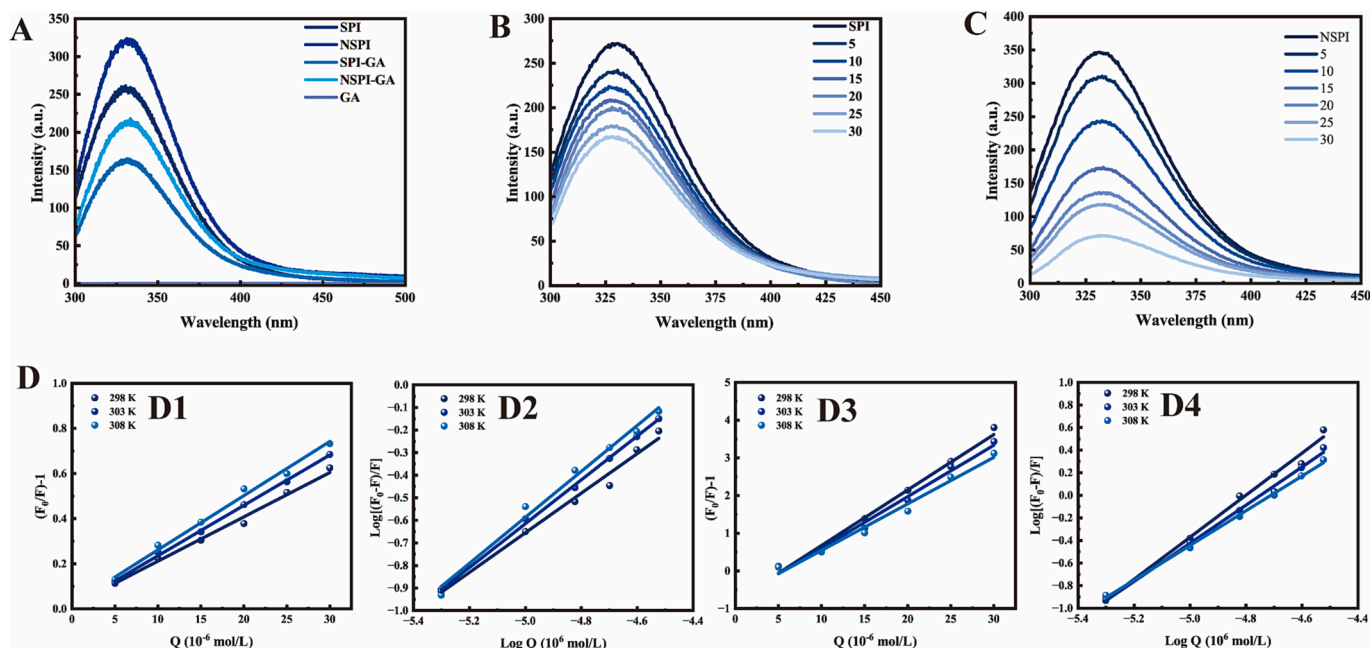


Fig. 2. (A) Fluorescence spectra of SPI, NSPI, and their complexes with GA at 298 K. Fluorescence spectra of SPI (B) and NSPI (C) quenched with different concentrations of GA at 298 K. The Stern–Volmer plots of SPI (D1) and NSPI (D3) quenched by GA at different temperatures. Double logarithmic regression plots of SPI (D2) and NSPI (D4) in the presence of GA at different temperatures.

skeleton, tryptophan, and tyrosine residues changed, possibly because of interactions between GA and residues in the polypeptide chain, thus changing the protein conformation and microenvironment of amino acid residues (Wang et al., 2021).

3.6.2. Intrinsic fluorescence quenching mechanism

To understand the possible interactions between SPI, NSPI, and GA, fluorescence quenching analysis was performed at different temperatures to investigate the binding modes of SPI/NSPI and GA. When excited at 280 nm, the intrinsic fluorescence of proteins is mainly induced by the fluorescence emission of Tyr and Trp residues, and a decrease in protein fluorescence intensity implies quenching of fluorophore interactions (Zhang et al., 2021). For SPI and NSPI, GA quenched the fluorescence intensity of the protein in a dose-dependent manner, indicating that the interaction between the protein and phenolic substances affected the protein fluorescence groups. Note that, compared to SPI, the addition of GA caused a red shift in the maximum emission wavelength of NSPI, indicating that the interaction between NSPI and GA modifies the peptide skeleton of the protein, resulting in a more hydrophilic microenvironment of amino acid residues that can interact with water molecules (W. Chen et al., 2019).

The fluorescence quenching mechanism can usually be divided into two modes, dynamic and static quenching, which can be determined by their different temperature dependencies (Wang et al., 2022). The Stern–Volmer equation was used for data analysis to explain the

quenching mechanism between proteins and small molecules. The Stern–Volmer plots of the GA-quenched SPI and NSPI at 298 K are shown in Fig. 2D1, 2D3, and the values of K_{SV} and K_q at different temperatures are shown in Table 2. For SPI, the K_{SV} value increase with temperature, whereas, for NSPI, the K_{SV} value decrease with temperature, and both have k_q values greater than the maximum collision quenching constant ($2.0 \times 10^{10} \text{ L mol}^{-1} \text{ s}^{-1}$). This indicates that both GA and SPI/NSPI underwent static quenching interactions (Zhang et al., 2021).

For the static quenching mechanism, the double logarithmic equation (Fig. 2D2, 2D4) was applied to characterize the mechanism of interaction between proteins and small molecules, and the results are listed in Table 2. For SPI, the calculated K_a values ranged from 3.729 to $4.504 \times 10^4 \text{ L mol}^{-1}$ with an n value of approximately 1, and for NSPI, the calculated K_a values ranges from 7.238 to $8.939 \times 10^4 \text{ L mol}^{-1}$ with an n value of approximately 2, indicating that the binding strength of GA to NSPI was superior to that of SPI, possibly because amination provided more amino groups for interaction with GA.

3.6.3. Binding driving force

To reveal the mechanism of interaction between SPI/NSPI and GA further, thermodynamic parameters were used to evaluate their interactions, as demonstrated in Table 2. Usually, when $\Delta H < 0$ or $\Delta H \approx 0$ and $\Delta S > 0$, electrostatic force is the main driving force, and when $\Delta H < 0$ and $\Delta S < 0$, van der Waals interactions or hydrogen bonds are the main driving factors, when $\Delta H > 0$ and $\Delta S > 0$, hydrophobic forces

Table 2
Thermodynamic parameters of the interaction between EGCG and SPI, NSPI.

Sample	T (K)	K_{SV} (10^4 L mol^{-1})	K_q ($10^{12} \text{ L mol}^{-1}$)	ΔH (kJ mol^{-1})	ΔS ($\text{J mol}^{-1}\text{K}^{-1}$)	ΔG (kJ mol^{-1})	K_a (10^4 M^{-1})	n	R^2
SPI	298	1.964 ± 0.00137^c	1.964 ± 0.00137^c	14.346 ± 0.12	59.081 ± 0.31	-3.361 ± 0.11^b	3.729 ± 0.262^b	0.877 ± 0.043^c	0.992
	303	2.234 ± 0.00051^b	2.234 ± 0.00051^b			-3.776 ± 0.13^a	4.241 ± 0.098^a	0.971 ± 0.025^b	0.997
	308	2.406 ± 0.00145^a	2.406 ± 0.00145^a			-3.851 ± 0.13^a	4.504 ± 0.275^a	1.018 ± 0.025^a	0.993
NSPI	298	1.472 ± 0.00971^A	1.472 ± 0.00971^A	-16.132 ± 0.14	36.317 ± 0.43	-26.954 ± 0.55^A	8.939 ± 0.433^A	1.862 ± 0.089^A	0.995
	303	1.364 ± 0.0086^B	1.364 ± 0.0086^B			-27.091 ± 0.49^A	8.016 ± 0.252^B	1.688 ± 0.052^B	0.996
	308	1.235 ± 0.00798^C	1.235 ± 0.00798^C			-27.317 ± 0.23^A	7.238 ± 0.174^C	1.536 ± 0.036^C	0.997

Note: Mean values with different superscript letters (a-c, A-C) in the same column indicate statistically significant differences ($p < 0.05$).

dominate (Yan, Xu, Zhang, Xie, et al., 2021). The ΔG values of all the samples were negative, confirming that the binding process was spontaneous. For SPI, because its $\Delta H > 0$ and $\Delta S > 0$, it can be presumed that it binds to GA mainly through hydrophobic interactions. In addition, concerning the enthalpy change ($\Delta H > 0$), K_a increased with the increase in temperature. For NSPI, because $\Delta H < 0$ and $\Delta S > 0$, it can be presumed that it binds to GA mainly through electrostatic interactions.

3.7. DSC

The thermal denaturation of proteins leads to conformational changes and the destruction of chemical interactions that maintain their structural integrity. The thermal stabilities of SPI, NSPI, and their complexes with polyphenols were analyzed using DSC, and the results are shown in Fig. 3A. Compared to SPI, NSPI exhibited a higher denaturation temperature, which may be attributed to conformational changes in NSPI, including molecular weight and additional branched side chains (Wang et al., 2019). After compounding with GA, the thermal denaturation temperature of both SPI-GA and NSPI-GA complexes decreased by about 5 °C, with SPI-GA showing the lowest denaturation temperature. This can be explained by the interaction between polyphenols and proteins, which alters the three-dimensional structure of the protein, resulting in a loose structure and a lower denaturation temperature (Feng et al., 2018). The above intrinsic fluorescence studies also demonstrate that SPI-GA has the lowest third-order conformational stability (Fig. 2A), which is consistent with the thermal stability results.

3.8. Surface hydrophobicity analysis

Surface hydrophobicity can reveal three-dimensional conformational and interface characteristic changes in proteins (Yan et al., 2021). Therefore, the surface hydrophobicity (H_0) of the proteins and their complexes was characterized using an external fluorescent probe, ANS, and the results are shown in Fig. 3B. Compared to SPI, amine grafting increased the surface hydrophobicity of NSPI. This aspect is attributed to two factors: (I) the stretching of the protein structure by the amine groups, which results in a decrease of the α -helix and β -turn content of the NSPI (Table 1), thus exposing more hydrophobic amino acids (Yan

et al., 2021). Zhu et al. (2020) also demonstrated that low α -helix and β -turn contents in the protein structure suggested a simultaneous improvement in flexibility and surface hydrophobicity. (II) Due to the grafting of a significant amount of amino groups, the ANS's site of action is expanded, resulting in higher fluorescence intensity (Wang et al., 2019). After complexation with GA, the exogenous fluorescence intensity of SPI-GA and NSPI-GA increased further, with NSPI-GA showing the highest fluorescence intensity possibly because the reaction of the protein with GA caused protein unfolding, resulting in the exposure of the internal hydrophobic clusters to the protein surface, thus increasing its surface hydrophobicity (Feng et al., 2018), as indicated by a decrease in the α -helix content of NSPI-GA (Table 1). Similar results were found by (D. Li et al., 2020), who demonstrated that the binding of catechins to protein residues stretched the protein and exposed more hydrophobic groups.

3.9. Analysis of emulsification characteristics

Emulsifying activity (EAI) refers to the ability of a protein to stabilize an oil–water interface, and emulsifying stability (ESI) refers to the strain capacity of the emulsion to form small droplets (O'Sullivan et al., 2016). The emulsification characteristics of SPI, NSPI, and their composites are shown in Fig. 3C. Compared to the SPI, the NSPI presented higher EAI and ESI values. This improvement may be due to the unfolding of the protein structure, which facilitates the formation of a stable interfacial layer at the oil–water interface and is characterized by changes in the secondary structure of NSPI, that is, a decrease in the-helix content and an increase in the random coil content. In addition, an increase in the surface hydrophobicity of proteins may also lead to an increase in the protein–lipid interactions, as well as the rearrangement of proteins at the oil–water interface, thus improving the stability of the emulsion (Yan, Xu, Zhang, & Li, 2021). Furthermore, the EAI and ESI of SPI and NSPI increased significantly after the protein was complexed with GA, which may be attributed to the increased flexibility of the protein structure and the increase in surface hydrophobicity due to GA. This allows a higher distribution of the protein at the oil–water interface, resulting in a thicker interfacial layer as well as promoting the interaction between protein molecules on the interfacial layer, thus increasing

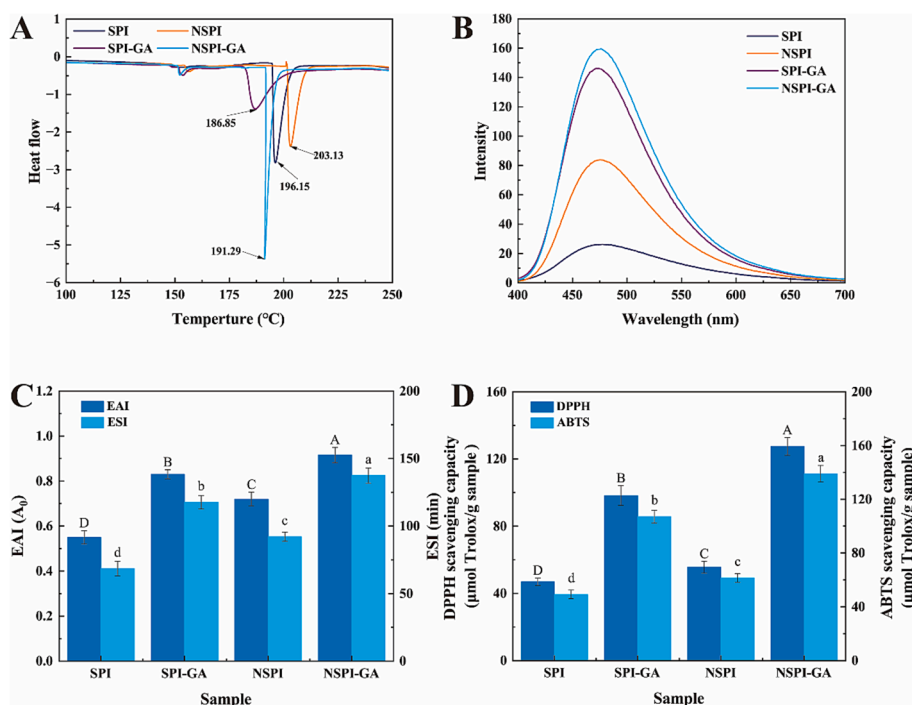


Fig. 3. Thermal stability (A), surface hydrophobicity (B), emulsifying activity index (C), and antioxidant activity (D) of SPI, NSPI, and their complexes with GA.

the density of the interfacial layer (Feng et al., 2018; Li et al., 2020; O'Sullivan et al., 2016).

3.10. Analysis of antioxidant properties

The DPPH and ABTS radical scavenging indices were used to characterize the antioxidant potential of the samples. The antioxidant capacity of the proteins was consistent with that previously reported (Fig. 3D), suggesting that proteins can chelate metal ions and, therefore, exhibit antioxidant properties (Yan et al., 2022). Compared to SPI, NSPI exhibits higher antioxidant properties. Possible mechanisms are (1) DPPH radicals can be more easily converted into stable DPPH-H molecules by accepting hydrogen atoms or free electrons from amino groups, (2) hydroxyl radicals can react with residual free NH_2 to form stable macromolecular radicals, and (3) amino groups have strong electron donating ability and may act as electron donors to convert Fe^{3+} into Fe^{2+} , (4) the modified protein has a higher sulfhydryl group content and, thus, exhibits better antioxidant properties (Bae et al., 2009; Yuan et al., 2022). After compounding with GA, SPI-GA and NSPI-GA both exhibited better antioxidant properties; in particular, NSPI-GA had the highest antioxidant activity, possibly because of the ability of phenolic hydroxyl groups to pair with DPPH single electrons, thereby scavenging free radicals. The phenolic hydroxyl groups of polyphenols became negatively charged after H ion loss and exhibited antioxidant properties through electrostatic interaction with ABTS (Sun et al., 2021).

4. Conclusion

The study involved grafting ethylenediamine (EDA) on a soybean protein isolate (SPI) through carbodiimide and complexing the resultant cationic soybean protein isolate (NSPI) with gallic acid (GA). The results reveal that EDA grafting improves positive charge, thermal stability, emulsifying, and antioxidant properties of SPI and that GA complexation further enhances these properties. Consequently, the NSPI-GA complex exhibited superior performance than the SPI-GA complex. The structural analysis indicates that EDA and GA induced conformational changes in SPI, reducing the α -helix content and increasing the random coil content. The binding mechanism analysis demonstrated that the interactions between SPI and GA were mainly hydrophobic, whereas those between NSPI and GA were electrostatic. Thus, NSPI has the potential to be an excellent carrier and enhancer of polyphenolic substances, which have various health benefits. However, the encapsulation performance, release ability, and potential toxicity of NSPI were not evaluated in this study. Therefore, these aspects should be explored, and the applicability of NSPI in food systems should be tested.

CRediT authorship contribution statement

Shizhang Yan: Methodology, Writing – original draft. **Qi Wang:** Software, Formal analysis. **Jiaye Yu:** Formal analysis. **Yang Li:** Funding acquisition. **Baokun Qi:** Supervision, Conceptualization, Writing – review & editing.

Declaration of Competing Interest

The authors declare that they have no known competing financial interests or personal relationships that could have appeared to influence the work reported in this paper.

Data availability

The authors do not have permission to share data.

Acknowledgments

We gratefully acknowledge the financial support received from the

National Soybean Industrial Technology System of China (CARS-04-PS32).

References

- Bae, M. J., Ishii, T., Minoda, K., Kawada, Y., Ichikawa, T., Mori, T., ... Nakayama, T. (2009). Albumin stabilizes (-)-epigallocatechin gallate in human serum: Binding capacity and antioxidant property. *Molecular Nutrition and Food Research*, 53(6), 709–715. <https://doi.org/10.1002/mnfr.200800274>
- Chen, H., Yu, S., Li, H., Wang, Z., Cai, P., Yang, Z., ... Guo, X. (2023). Conjugation of aminated sugar beet pectin-tannic acid nanoparticles with cinnamaldehyde at the oil-water interface to stabilize a 3D printable high-internal phase emulsion. *Food Hydrocolloids*, 144, Article 108937. <https://doi.org/10.1016/j.foodhyd.2023.108937>
- Chen, H., Wang, Z., Guo, X., Yu, S., Zhang, T., Tang, X., ... Meng, H. (2022). Tannic acid-aminated sugar beet pectin nanoparticles as a stabilizer of high-internal-phase Pickering emulsions. *Journal of Agricultural and Food Chemistry*, 70(26), 8052–8063. <https://doi.org/10.1021/acs.jafc.1c04865>
- Chen, W., Wang, W., Ma, X., Lv, R., Balaso Watharkar, R., Ding, T., ... Liu, D. (2019). Effect of pH-shifting treatment on structural and functional properties of whey protein isolate and its interaction with (-)-epigallocatechin-3-gallate. *Food Chemistry*, 274, 234–241. <https://doi.org/10.1016/j.foodchem.2018.08.106>
- Dai, S., Liao, P., Wang, Y., Tian, T., Tong, X., Lyu, B., ... Wang, H. (2023). Soy protein isolate-catechin non-covalent and covalent complexes: Focus on structure, aggregation, stability and in vitro digestion characteristics. *Food Hydrocolloids*, 135, Article 108108. <https://doi.org/10.1016/j.foodhyd.2022.108108>
- Feng, J., Cai, H., Wang, H., Li, C., & Liu, S. (2018). Improved oxidative stability of fish oil emulsion by grafted ovalbumin-catechin conjugates. *Food Chemistry*, 241, 60–69. <https://doi.org/10.1016/j.foodchem.2017.08.055>
- Jiang, J., Chen, J., & Xiong, Y. L. (2009). Structural and emulsifying properties of soy protein isolate subjected to acid and alkaline pH-shifting processes. *Journal of Agricultural and Food Chemistry*, 57(16), 7576–7583. <https://doi.org/10.1021/jf901585n>
- Jin, S., Li, K., Gao, Q., Zhang, W., Chen, H., Li, J., & Shi, S. Q. (2020). Multiple crosslinking strategy to achieve high bonding strength and antibacterial properties of double-network soy adhesive. *Journal of Cleaner Production*, 254, Article 120143. <https://doi.org/10.1016/j.jclepro.2020.120143>
- Li, D., Zhao, Y., Wang, X., Tang, H., Wu, N., Wu, F., ... Elfalleh, W. (2020). Effects of (+)-catechin on a rice bran protein oil-in-water emulsion: Droplet size, zeta-potential, emulsifying properties, and rheological behavior. *Food Hydrocolloids*, 98, Article 105306. <https://doi.org/10.1016/j.foodhyd.2019.105306>
- Li, H., Pan, Y., Yang, Z., Rao, J., & Chen, B. (2022). Modification of β -lactoglobulin by phenolic conjugations: Protein structural changes and physicochemical stabilities of stripped hemp oil-in-water emulsions stabilized by the conjugates. *Food Hydrocolloids*, 128, Article 107578. <https://doi.org/10.1016/j.foodhyd.2022.107578>
- Likitdecharoj, P., & Ratanavaraporn, J. (2018). Comparative study in physico-chemical properties of gelatin derivatives and their microspheres as carriers for controlled release of green tea's extract. *Journal of Drug Delivery Science and Technology*, 47, 367–374. <https://doi.org/10.1016/j.jddst.2018.08.005>
- Mohammadi, A., Kashi, P. A., Kashiri, M., Bagheri, A., Chen, J., Ettelaie, R., ... Shahbazi, M. (2023). Self-assembly of plant polyphenols-grafted soy proteins to manufacture a highly stable antioxidative Pickering emulsion gel for direct-ink-write 3D printing. *Food Hydrocolloids*, 142, Article 108851. <https://doi.org/10.1016/j.foodhyd.2023.108851>
- O'Sullivan, J., Murray, B., Flynn, C., & Norton, I. (2016). The effect of ultrasound treatment on the structural, physical and emulsifying properties of animal and vegetable proteins. *Food Hydrocolloids*, 53, 141–154. <https://doi.org/10.1016/j.foodhyd.2015.02.009>
- Pi, X., Liu, J., Sun, Y., Ban, Q., Cheng, J., & Guo, M. (2023). Protein modification, IgE binding capacity, and functional properties of soybean protein upon conjugation with polyphenols. *Food Chemistry*, 405, Article 134820. <https://doi.org/10.1016/j.foodchem.2022.134820>
- Pi, X., Sun, Y., Liu, J., Wang, X., Hong, W., Cheng, J., & Guo, M. (2023). Characterization of the improved functionality in soybean protein-proanthocyanidins conjugates prepared by the alkali treatment. *Food Hydrocolloids*, 134, Article 108107. <https://doi.org/10.1016/j.foodhyd.2022.108107>
- Sarika, P. R., & James, N. R. (2016). Polyelectrolyte complex nanoparticles from carboxymethylated gelatin and sodium alginate for curcumin delivery. *Carbohydrate Polymers*, 148, 354–361. <https://doi.org/10.1016/j.carbpol.2016.04.073>
- Sarika, P. R., Pavithran, A., & James, N. R. (2015). Cationized gelatin/gum Arabic polyelectrolyte complex: Study of electrostatic interactions. *Food Hydrocolloids*, 49, 176–182. <https://doi.org/10.1016/j.foodhyd.2015.02.039>
- Sui, X., Sun, H., Qi, B., Zhang, M., Li, Y., & Jiang, L. (2018). Functional and conformational changes to soy proteins accompanying anthocyanins: Focus on covalent and non-covalent interactions. *Food Chemistry*, 245, 871–878. <https://doi.org/10.1016/j.foodchem.2017.11.090>
- Sun, C., Zeng, X., Zheng, S., Wang, Y., Li, Z., Zhang, H., ... Yang, X. (2021). Bio-adhesive catechol-modified chitosan wound healing hydrogel dressings through glow discharge plasma technique. *Chemical Engineering Journal*, 427, Article 130843. <https://doi.org/10.1016/j.cej.2021.130843>
- Tan, H., Zhang, R., Han, L., Zhang, T., & Ngai, T. (2022). Pickering emulsions stabilized by aminated gelatin nanoparticles: Are gelatin nanoparticles acting as genuine Pickering stabilizers or structuring agents? *Food Hydrocolloids*, 123, Article 107151. <https://doi.org/10.1016/j.foodhyd.2021.107151>

- Teng, Z., Li, Y., Niu, Y., Xu, Y., Yu, L., & Wang, Q. (2014). Cationic β -lactoglobulin nanoparticles as a bioavailability enhancer: Comparison between ethylenediamine and polyethyleneimine as cationizers. *Food Chemistry*, 159, 333–342. <https://doi.org/10.1016/j.foodchem.2014.03.022>
- Wang, C., Chen, L., Lu, Y., Liu, J., Zhao, R., Sun, Y., ... Cuina, W. (2021). pH-Dependent complexation between β -lactoglobulin and lycopene: Multi-spectroscopy, molecular docking and dynamic simulation study. *Food Chemistry*, 362, Article 130230. <https://doi.org/10.1016/j.foodchem.2021.130230>
- Wang, H., You, S., Wang, W., Zeng, Y., Su, R., Qi, W., ... He, Z. (2022). Laccase-catalyzed soy protein and gallic acid complexation: Effects on conformational structures and antioxidant activity. *Food Chemistry*, 375, Article 131865. <https://doi.org/10.1016/j.foodchem.2021.131865>
- Wang, Q., Tang, Y., Yang, Y., Lei, L., Lei, X., Zhao, J., ... Ming, J. (2022). The interaction mechanisms, and structural changes of the interaction between zein and ferulic acid under different pH conditions. *Food Hydrocolloids*, 124, Article 107251. <https://doi.org/10.1016/j.foodhyd.2021.107251>
- Wang, W., Dong, X., & Sun, Y. (2019). Modification of serum albumin by high conversion of carboxyl to amino groups creates a potent inhibitor of amyloid β -protein fibrillogenesis. *Bioconjugate Chemistry*, 30(5), 1477–1488. <https://doi.org/10.1021/acs.bioconjchem.9b00209>
- Yan, S., Xie, F., Zhang, S., Jiang, L., Qi, B., & Li, Y. (2021). Effects of soybean protein isolate – polyphenol conjugate formation on the protein structure and emulsifying properties: Protein – polyphenol emulsification performance in the presence of chitosan. *Colloids and Surfaces A: Physicochemical and Engineering Aspects*, 609, Article 125641. <https://doi.org/10.1016/j.colsurfa.2020.125641>
- Yan, S., Xu, J., Zhang, S., & Li, Y. (2021). Effects of flexibility and surface hydrophobicity on emulsifying properties: Ultrasound-treated soybean protein isolate. *Lwt*, 142, Article 110881. <https://doi.org/10.1016/j.lwt.2021.110881>
- Yan, S., Xu, J., Zhang, X., Xie, F., Zhang, S., Jiang, L., ... Li, Y. (2021). Effect of pH-shifting treatment on the structural and functional properties of soybean protein isolate and its interactions with (–)-epigallocatechin-3-gallate. *Process Biochemistry*, 101, 190–198. <https://doi.org/10.1016/j.procbio.2020.10.016>
- Yan, S., Yao, Y., Xie, X., Zhang, S., Huang, Y., Zhu, H., ... Qi, B. (2022). Comparison of the physical stabilities and oxidation of lipids and proteins in natural and polyphenol-modified soybean protein isolate-stabilized emulsions. *Food Research International*, 162, Article 112066. <https://doi.org/10.1016/j.foodres.2022.112066>
- Yi, F., Wu, K., Yu, G., & Su, C. (2021). Preparation of Pickering emulsion based on soy protein isolate-gallic acid with outstanding antioxidation and antimicrobial. *Colloids and Surfaces B: Biointerfaces*, 206, Article 111954. <https://doi.org/10.1016/j.colsurfb.2021.111954>
- Yuan, Y., Tan, W., Zhang, J., Li, Q., & Guo, Z. (2022). Water-soluble amino functionalized chitosan: Preparation, characterization, antioxidant and antibacterial activities. *International Journal of Biological Macromolecules*, 217, 969–978. <https://doi.org/10.1016/j.ijbiomac.2022.07.187>
- Zeng, Y., Yang, W., Xu, P., Cai, X., Dong, W., Chen, M., ... Ma, P. (2022). The bonding strength, water resistance and flame retardancy of soy protein-based adhesive by incorporating tailor-made core-shell nanohybrid compounds. *Chemical Engineering Journal*, 428, Article 132390. <https://doi.org/10.1016/j.cej.2021.132390>
- Zhang, Q., Li, H., Cen, C., Zhang, J., Wang, S., Wang, Y., & Fu, L. (2021). Ultrasonic pretreatment modifies the pH-dependent molecular interactions between β -lactoglobulin and dietary phenolics: Conformational structures and interfacial properties. *Ultrasonics Sonochemistry*, 75, Article 105612. <https://doi.org/10.1016/j.ultrsonch.2021.105612>
- Zhou, S. D., Lin, Y. F., Xu, X., Meng, L., & Dong, M. S. (2020). Effect of non-covalent and covalent complexation of (–)-epigallocatechin gallate with soybean protein isolate on protein structure and in vitro digestion characteristics. *Food Chemistry*, 309, Article 125718. <https://doi.org/10.1016/j.foodchem.2019.125718>
- Zhou, X., Wu, Y., Zhou, X., Huang, Z., Zhao, L., & Liu, C. (2022). Elaboration of cationic soluble soybean polysaccharides-epigallocatechin gallate nanoparticles with sustained antioxidant and antimicrobial activities. *Journal of Agricultural and Food Chemistry*, 70(36), 11353–11366. <https://doi.org/10.1021/acs.jafc.2c03510>
- Zhu, Y., Fu, S., Wu, C., Qi, B., Teng, F., Wang, Z., ... Jiang, L. (2020). The investigation of protein flexibility of various soybean cultivars in relation to physicochemical and conformational properties. *Food Hydrocolloids*, 103, Article 105709. <https://doi.org/10.1016/j.foodhyd.2020.105709>